The modRSW model – physical basis, numerics, and dynamics

Tom Kent*
Work with: Onno Bokhove*, Steven Tobias*, Gordon Inverarity[†]

*Dept. of Applied Maths, University of Leeds
[†]Met Office, Exeter

Email: t.kent@leeds.ac.uk

DA workshop, Leeds – May 2019

NWP and DA: from large- to convective-scale to 'idealised'

DA techniques need to evolve in order to keep up with the developments in high-resolution NWP

- increasing resolution is not a panacea: 'grey zone' presents many problems...
- more (nonlinear) dynamical processes such as convection, cloud formation, and small-scale gravity waves, are resolved explicitly/partially
- breakdown of dynamical balances (e.g., hydrostatic and geostrophic) at smaller scales
- ensemble-based methods: flow-dependent errors

NWP and DA: from large- to convective-scale to 'idealised'

DA techniques need to evolve in order to keep up with the developments in high-resolution NWP

- increasing resolution is not a panacea: 'grey zone' presents many problems...
- more (nonlinear) dynamical processes such as convection, cloud formation, and small-scale gravity waves, are resolved explicitly/partially
- breakdown of dynamical balances (e.g., hydrostatic and geostrophic) at smaller scales
- ensemble-based methods: flow-dependent errors

It may be unfeasible, and indeed undesirable, to investigate the potential of DA schemes on state-of-the-art NWP models. Instead idealised models can be employed that:

- capture some fundamental processes
- are computationally inexpensive to implement

E.g., 'Idealised' models: hierarchy of complexity

- Lorenz (L63, L95, L2005, ...)
- **SW**/BV/QG models
- simplified NWP models

Using idealised models: approach

1. introduce a physically plausible idealised model and implement numerically
   - Kent et al. (2017): based on the rotating shallow water equations (SWEs) and extending the model of Würsch and Craig (2014) for simplified cumulus cloud dynamics
   - investigate dynamics of the modified model and compare to those of the classical shallow water theory

2. ensemble-based DA - relevant for convective-scale NWP?
   - algorithm: (deterministic) EnKF with techniques to combat sampling errors
   - for relevant experiments:
     - dynamics: set-up, time- and length-scales, ...
     - assimilation: tuning the observing system and ensemble configuration in search of a 'well-tuned' experiment.
     - diagnostics: error-spread statistics, CRPS, observational influence, error-growth statistics...

Houtekamer and Zhang (2016): "*The frontier of data assimilation is at the high spatial and temporal resolution, where we have rapidly developing precipitating systems with complex dynamics*".

An idealised model of convective-scale NWP

Moist convection... *is many things* (Stevens 2005)

- Manifest as clouds, it comprises a variety of regimes spanning a vast range of spatial and temporal scales, with diverse and nonlinear physical processes in each regime...
- state-of-the-art numerical models of the atmosphere struggle with their treatment of moist convection
- we seek to represent some of the fundamental processes and aspects of moist convection in a relatively simple modelling environment.

An idealised model of convective-scale NWP

Moist convection... *is many things* (Stevens 2005)

- Manifest as clouds, it comprises a variety of regimes spanning a vast range of spatial and temporal scales, with diverse and nonlinear physical processes in each regime...
- state-of-the-art numerical models of the atmosphere struggle with their treatment of moist convection
- we seek to represent some of the fundamental processes and aspects of moist convection in a relatively simple modelling environment.

Idealised model: concept

- *"It is almost as if the fluid is magically transformed into another form once it crosses a certain threshold..."* (Stevens again)
- "*moist convection can in many instances be thought of as a two-fluid problem, where one fluid (unsaturated air) can transform itself into another (saturated air) simply through vertical displacement.*"
- Würsch and Craig (2014) model: the single–layer shallow water equations are modified when the height of the fluid crosses certain thresholds
- the behaviour of the flow is transformed from the standard shallow water dynamics to a simplified representation of convection, with associated precipitation effects

1. SWEs: an extension

$1.5D$ rotating SWEs on an f-plane with no variation in the y-direction ($\partial_y = 0$):

$$\partial_t h + \partial_x(hu) = 0,$$
$$\partial_t(hu) + \partial_x(hu^2 + p(h)) - fhv = -gh\partial_x b,$$
$$\partial_t(hv) + \partial_x(huv) + fhu = 0,$$

where $p(h)$ is an effective pressure: $p(h) = \frac{1}{2}gh^2$.

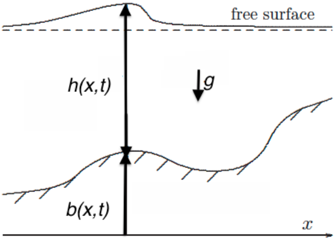

Aim: modify the SWEs to include more complex dynamics relevant for the 'convective-scale', based on the model of Würsch and Craig (2014)

- convective updrafts - artificially mimic conditional instability (positive buoyancy)
- idealised representation of precipitation ('rain' mass fraction), including source and sink
- switches for the onset of convection and precipitation - realistic (and highly nonlinear) features of operational NWP models

Modified SWEs

- two threshold heights $H_c < H_r$: when fluid exceeds these heights, different mechanisms kick in and alter the classical SW dynamics
- modifications to the effective pressure gradient (via SW pressure: $p(h) = \frac{1}{2}gh^2$) in the momentum equation
- extra equation for the conservation of model 'rain' to close the system

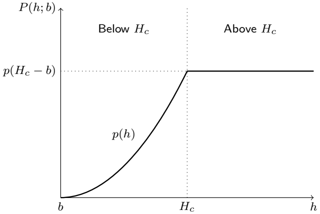

Modified pressure $P(h;b)$: $p(H_c - b) = \frac{1}{2}g(H_c - b)^2$ above the threshold H_c is lower than the standard pressure $p(h) = \frac{1}{2}gh^2$, thus forcing the fluid to rise where $h + b > H_c$.

$$\partial_t h + \partial_x(hu) = 0,$$

$$\partial_t(hu) + \partial_x(hu^2 + P) + hc_0^2\partial_x r - fhv = -Q\partial_x b,$$

$$\partial_t(hv) + \partial_x(huv) + fhu = 0,$$

$$\partial_t(hr) + \partial_x(hur) + h\widetilde{\beta}\partial_x u + \alpha hr = 0,$$

where
$$P = P(h;b) = \begin{cases} p(H_c - b), & \text{for } h + b > H_c, \\ p(h), & \text{otherwise,} \end{cases}$$

$$Q = Q(h;b) = \begin{cases} p'(H_c - b), & \text{for } h + b > H_c, \\ p'(h), & \text{otherwise,} \end{cases}$$

and
$$\widetilde{\beta} = \begin{cases} \beta, & \text{for } h + b > H_r,\ \partial_x u < 0, \\ 0, & \text{otherwise.} \end{cases}$$

Modified SWEs

- two threshold heights $H_c < H_r$: when fluid exceeds these heights, different mechanisms kick in and alter the classical SW dynamics
- modifications to the effective pressure gradient (via SW pressure: $p(h) = \frac{1}{2}gh^2$) in the momentum equation
- extra equation for the conservation of model 'rain' to close the system

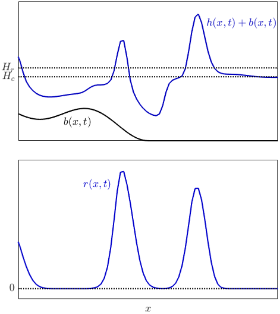

Schematic solutions: convection (in h field) and associated 'rain'

$$\partial_t h + \partial_x (hu) = 0,$$

$$\partial_t (hu) + \partial_x (hu^2 + P) + hc_0^2 \partial_x r - fhv = -Q\partial_x b,$$

$$\partial_t (hv) + \partial_x (huv) + fhu = 0,$$

$$\partial_t (hr) + \partial_x (hur) + h\widetilde{\beta}\partial_x u + \alpha hr = 0,$$

where $P = P(h;b) = \begin{cases} p(H_c - b), & \text{for } h + b > H_c, \\ p(h), & \text{otherwise,} \end{cases}$

$$Q = Q(h;b) = \begin{cases} p'(H_c - b), & \text{for } h + b > H_c, \\ p'(h), & \text{otherwise,} \end{cases}$$

and $\widetilde{\beta} = \begin{cases} \beta, & \text{for } h + b > H_r,\ \partial_x u < 0, \\ 0, & \text{otherwise.} \end{cases}$

Some theoretical aspects

Eigenanalysis: shallow water systems are hyperbolic, and can thus be solved via a range of numerical recipes for hyperbolic systems. What about the modified system?

$$\partial_t \boldsymbol{U} + \partial_x \boldsymbol{F}(\boldsymbol{U}) + \boldsymbol{G}(\boldsymbol{U})\partial_x \boldsymbol{U} + \boldsymbol{S}(\boldsymbol{U}) = 0,$$

Hyperbolicity determined by eigen-structure: (all eigenvalues must be real). Eigenvalues of the system are determined by the Jacobian matrix $\partial \boldsymbol{F}/\partial \boldsymbol{U} + \boldsymbol{G}(\boldsymbol{U})$:

$$\lambda_{1,2} = u \pm \sqrt{\partial_h P + c_0^2 \widetilde{\beta}}, \quad \lambda_{3,4} = u.$$

Since $P(h;b)$ is non-decreasing and $\widetilde{\beta}$ non-negative, the eigenvalues are real. Hence, the modified SW model is (weakly) hyperbolic.

Some theoretical aspects

Eigenanalysis: shallow water systems are hyperbolic, and can thus be solved via a range of numerical recipes for hyperbolic systems. What about the modified system?

$$\partial_t \boldsymbol{U} + \partial_x \boldsymbol{F}(\boldsymbol{U}) + \boldsymbol{G}(\boldsymbol{U})\partial_x \boldsymbol{U} + \boldsymbol{S}(\boldsymbol{U}) = 0,$$

Hyperbolicity determined by eigen-structure: (all eigenvalues must be real).
Eigenvalues of the system are determined by the Jacobian matrix $\partial \boldsymbol{F}/\partial \boldsymbol{U} + \boldsymbol{G}(\boldsymbol{U})$:

$$\lambda_{1,2} = u \pm \sqrt{\partial_h P + c_0^2 \widetilde{\beta}}, \quad \lambda_{3,4} = u.$$

Since $P(h;b)$ is non-decreasing and $\widetilde{\beta}$ non-negative, the eigenvalues are real. Hence, the modified SW model is (weakly) hyperbolic.

Wave speeds: waves travelling through (saturated) regions of convection slow down

- $h + b < H_c$: $\partial_h P = gh$, $\widetilde{\beta} = 0$ implies standard eigenvalues $\lambda_{1,2} = u \pm \sqrt{gh}$
- $H_c < h + b < H_r$: $\partial_h P = 0$, $\widetilde{\beta} = 0$ implies modified eigenvalues $\lambda_{1,2} = u$
- $H_r < h + b$: $\partial_h P = 0$ and $\widetilde{\beta} = \beta$ implies modified eigenvalues $\lambda_{1,2} = u \pm \sqrt{c_0^2 \beta}$

Numerics

Methodology:

- Rhebergen et al. (2008): a novel discontinuous Galerkin (DG) finite element framework for non-conservative hyperbolic system of PDEs, deals robustly with high nonlinearity and non-conservative products, $\boldsymbol{G}(\boldsymbol{U})\partial_x \boldsymbol{U}$
- combine with the scheme of Audusse et al. (2004) to discretise topography: maintains well-balancedness and preserves non-negativity of fluid depth and 'rain'
- discretises the flow domain into N_{el} elements (defining the horizontal resolution of the model) and uses a dynamic time-step that guarantees stability while allowing for gains in efficiency (i.e., a larger time step) when possible.

Numerics

Methodology:

- Rhebergen et al. (2008): a novel discontinuous Galerkin (DG) finite element framework for non-conservative hyperbolic system of PDEs, deals robustly with high nonlinearity and non-conservative products, $\boldsymbol{G}(\boldsymbol{U})\partial_x \boldsymbol{U}$
- combine with the scheme of Audusse et al. (2004) to discretise topography: maintains well-balancedness and preserves non-negativity of fluid depth and 'rain'
- discretises the flow domain into N_{el} elements (defining the horizontal resolution of the model) and uses a dynamic time-step that guarantees stability while allowing for gains in efficiency (i.e., a larger time step) when possible.

Experiments: based on (i) a Rossby adjustment scenario, and (ii) non-rotating flow over topography. To illustrate the effect that exceeding the threshold heights $H_c < H_r$ has on the dynamics, a hierarchy of model 'cases' is employed:

- Case I: $h + b < H_c$ always (effectively setting $H_c, H_r \to \infty$). The model reduces to standard RSWEs if $hr = 0$ initially.
- Case II: $h + b < H_r$ always, but may exceed H_c. This is considered a 'stepping stone' to the full model to isolate the effect of the first threshold exceedance.
- Case III: $h + b$ may exceed both H_c, H_r. This is the idealised fluid model with convection and rain processes to be used for convective-scale DA experiments.

Solve non–dimensionalised equations, with 2 prognostic parameters: Ro and Fr.

(i) Rossby adjustment scenario

- rotating flow $(\mathrm{Ro} = 0.1, \mathrm{Fr} = 1)$ with flat bottom topography $(b \equiv 0)$
- the free surface height h is disturbed from its rest state by a transverse jet, i.e., fluid with an initial constant height profile is subject to a localised v-velocity distribution
- to adjust to this initial momentum imbalance, the height field evolves rapidly, emitting inertia gravity waves and shocks that propagate out from the jet and eventually reach a state of geostrophic balance.

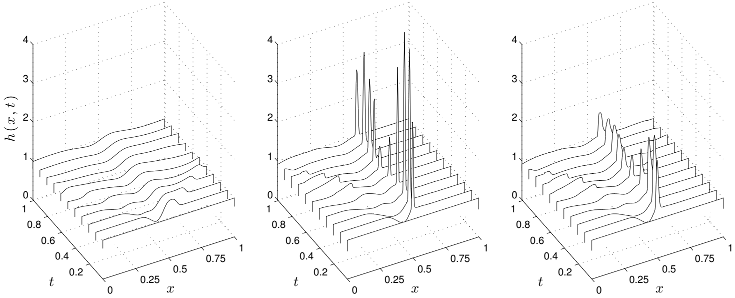

Figure: Time evolution of the height profile: case I (left), II (middle), III (right).

Snapshots of $h(x,t)$ and $r(x,t)$ for the Rossby adjustment process with initial transverse jet $(\mathrm{Ro} = 0.1, \mathrm{Fr} = 1)$:

- case I (left), II (middle), and III (right)
- Top row: Hovmöller plots for h
- Subsequent rows: profiles of h (black line; left axis) and r (blue line; right axis) at different times denoted by the dashed lines in the top row

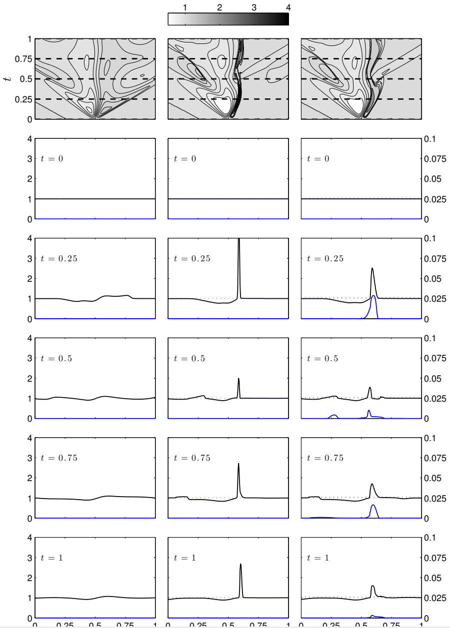

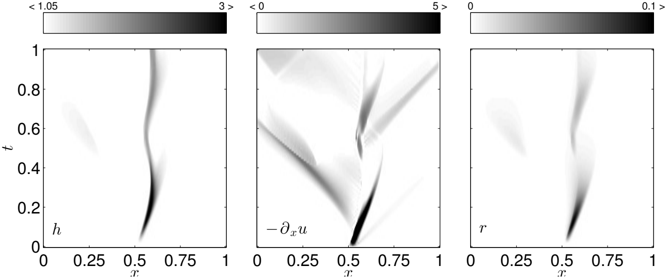

Hovmöller plots for the Rossby adjustment process with initial transverse jet $(\mathrm{Ro} = 0.1, \mathrm{Fr} = 1)$, highlighting the conditions for the production of rain: case III. From left to right: $h > H_r$, $-\partial_x u > 0$, and $r(x, t)$.

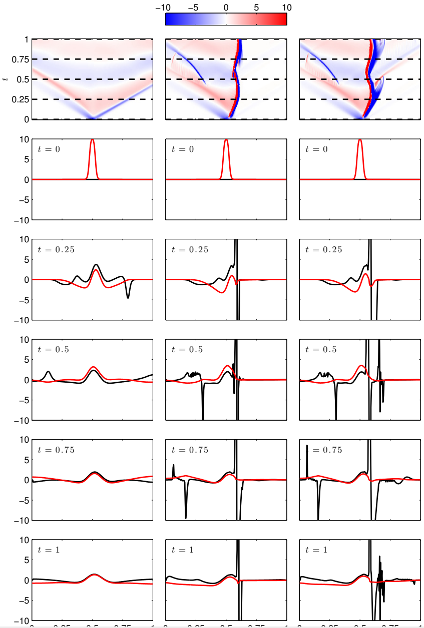

- Top row: Hovmöller diagram plotting the evolution of the measure of departure from geostrophic balance $g\partial_x h - fv$: light shading denotes regions close to geostrophic balance
- Subsequent rows: profiles of fv (red) and $g\partial_x h$ (black) at different times denoted by the dashed lines in the top row
- case I (left), II (middle), and III (right)

(ii) Flow over topography

Consider non-rotating flow (no transverse velocity) over a parabolic ridge:

$$b(x) = \begin{cases} b_c \left(1 - \left(\frac{x-x_p}{a}\right)^2\right), & \text{for } |x - x_p| \leq a; \\ 0, & \text{otherwise;} \end{cases}$$

where b_c is the height of the hill crest, a is the hill width parameter, and x_p its location in the domain.

- shallow water flow over topography has been extensively researched
- often used as a test case in numerical studies owing to the range of dynamics (dependent on Froude number Fr), including shocks, and the existence of analytical non-trivial steady state solutions
- supercritical flow $\mathrm{Fr} > 1$: the fluid depth increases over the ridge (as opposed to subcritical flow ($\mathrm{Fr} < 1$) in which the depth decreases over the ridge) and a shock wave propagates at a height above the rest depth to the right of the ridge

Flow over topography ($\mathrm{Fr} = 2$, $b_c = 0.5$, $a = 0.05$, and $x_p = 0.1$):

- profiles of $h + b$, b (black; left y-axis), rain r (blue; right y-axis), and exact steady-state solution for $h + b$ (red dashed) at different times
- case I (left), II (middle), and III (right)
- dotted lines denote the threshold heights for convection and rain $H_c < H_r$

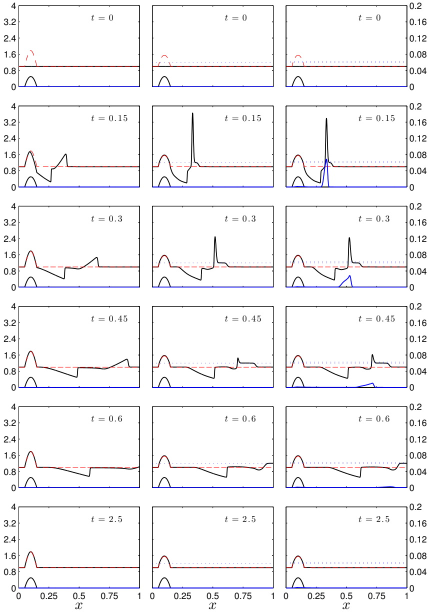

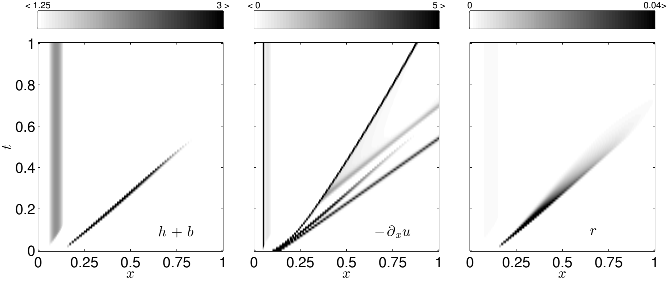

Hovmöller plots for flow over topography $(\mathrm{Fr} = 2)$, highlighting the conditions for the production and subsequent evolution of rain: case III. From left to right: $h + b > H_r$, $-\partial_x u > 0$, and $r(x, t)$.

Flow over topography ($\mathrm{Fr} = 2$, $b_c = 0.4$, $a = 0.05$, $(x_{p_1}, x_{p_2}) = (0.0875, 0.2625)$:

- profiles of $h + b$, b (black; left y-axis), rain r (blue; right y-axis), and exact steady-state solution for $h + b$ (red dashed) at different times
- case I (left), II (middle), and III (right)
- dotted lines denote the threshold heights for convection and rain $H_c < H_r$

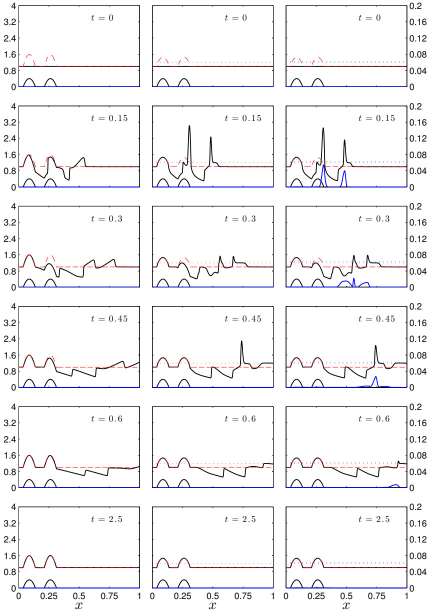

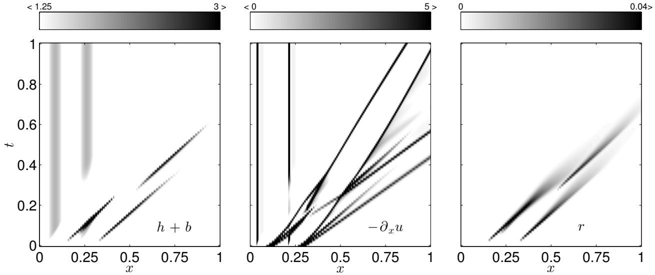

Hovmöller plots for flow over two ridges ($\mathrm{Fr} = 2$), highlighting the conditions for the production and subsequent evolution of rain: case III. From left to right: $h + b > H_r$, $-\partial_x u > 0$, and $r(x, t)$.

Dynamics: summary

- changes to the dynamics are brought about by the exceedance of two threshold heights H_c and H_r, akin to (i) the level of free convection, and (ii) the onset of precipitation
- when the fluid exceeds these heights, the classical shallow water dynamics are altered to include a representation of conditional instability (leading to a convective updraft) and idealised moisture transport with associated downdraft and precipitation effects
- the model reduces exactly to the standard SWEs in non-convecting, non-precipitating regions

Dynamics: summary

- changes to the dynamics are brought about by the exceedance of two threshold heights H_c and H_r, akin to (i) the level of free convection, and (ii) the onset of precipitation
- when the fluid exceeds these heights, the classical shallow water dynamics are altered to include a representation of conditional instability (leading to a convective updraft) and idealised moisture transport with associated downdraft and precipitation effects
- the model reduces exactly to the standard SWEs in non-convecting, non-precipitating regions
- the model also exhibits important aspects of convective-scale dynamics relating to the disruption of large-scale balance principles
  - Rossby adjustment scenario illustrates the breakdown of geostrophic balance in the presence of convection and precipitation
  - breakdown of hydrostatic balance is implicity enforced by the modified pressure when the level of free convection is exceeded
- able to simulate other features related to convecting and precipitating weather systems, such as the initiation of daughter cells away from the parent cell by gravity wave propagation, and convection downstream from an orographic ridge.

GitHub repository: modRSW_EnKF

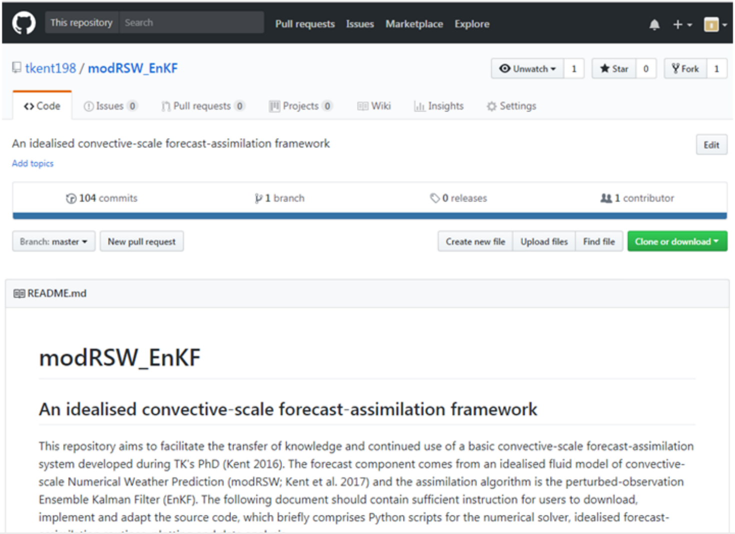

Thanks very much for your attention ... questions?

References:

- Kent, Bokhove, & Tobias (2017): **Dynamics of an idealized fluid model for investigating convective-scale data assimilation**. *Tellus A: Dynamic Meteorology and Oceanography*, 69(1), 1369332
- Kent (2017): **'An idealised convective-scale forecast-assimilation framework'**, `https://github.com/tkent198/modRSW_EnKF`
- Audusse et al., (2004): A fast and stable well-balanced scheme with hydrostatic reconstruction for shallow water flows. *SIAM JSC*, 25(6), 2050-2065.
- Houtekamer, P.L. and Zhang, F. (2016): Review of the Ensemble Kalman Filter for Atmospheric Data Assimilation, *MWR (Early Online Release)*, DOI: http://dx.doi.org/10.1175/MWR-D-15-0440.1
- Rhebergen, S., Bokhove, O., and Van der Vegt, J., (2008): Discontinuous Galerkin finite element methods for hyperbolic nonconservative partial differential equations. *J. Comp. Phys.*, 227(3), 1887-1922.
- Stevens, B. (2005): Atmospheric moist convection. *Annu. Rev. Earth Planet. Sci.*, 33, 605-643.
- Würsch, M., and Craig, G.C., (2014): A simple dynamical model of cumulus convection for data assimilation research. *Meteorologische Zeitschrift*, 23(5):483-490.

Non-dimensionalised modRSW equations

$$
\begin{aligned}
&\partial_t h + \partial_x (hu) = 0,\\
&\partial_t (hu) + \partial_x (hu^2 + P) + Q\partial_x b + h\widetilde{c_0}^2 \partial_x r - \frac{1}{\mathrm{Ro}} hv = 0,\\
&\partial_t (hv) + \partial_x (huv) + \frac{1}{\mathrm{Ro}} hu = 0,\\
&\partial_t (hr) + \partial_x (hur) + h\widetilde{\beta}\partial_x u + \widetilde{\alpha} hr = 0,
\end{aligned}
$$

where:

$$
\begin{aligned}
P(h,b) &= \frac{1}{2\mathrm{Fr}^2}\left[h^2 + ((H_c - b)^2 - h^2)\Theta(h + b - H_c)\right],\\
Q(h,b) &= \frac{1}{\mathrm{Fr}^2}\left[h + (H_c - b - h)\Theta(h + b - H_c)\right],\\
\widetilde{\beta} &= \beta\Theta(h + b - H_r)\Theta(-\partial_x u).
\end{aligned}
$$

$\Theta(x) = 1$ if $x > 0$; and 0 if $x \leq 0$, and the following parameters are introduced:

$$
\mathrm{Fr} = \frac{V_0}{\sqrt{gH_0}}, \qquad \mathrm{Ro} = \frac{V_0}{fL_0}, \qquad \widetilde{c_0}^2 = \frac{c_0^2}{V_0^2}, \qquad \widetilde{\alpha} = \frac{L_0}{V_0}\alpha.
$$

Some theoretical aspects

- Shallow water systems are hyperbolic, and can thus be solved via a range of numerical recipes for hyperbolic syststems. What about the modified system?

$$\partial_t \boldsymbol{U} + \partial_x \boldsymbol{F}(\boldsymbol{U}) + \boldsymbol{G}(\boldsymbol{U})\partial_x \boldsymbol{U} + \boldsymbol{S}(\boldsymbol{U}) = 0,$$

where:

$$\boldsymbol{U} = \begin{bmatrix} h \\ hu \\ hv \\ hr \end{bmatrix}, \boldsymbol{F}(\boldsymbol{U}) = \begin{bmatrix} hu \\ hu^2 + P \\ huv \\ hur \end{bmatrix}, \boldsymbol{G}(\boldsymbol{U}) = \begin{bmatrix} 0 & 0 & 0 & 0 \\ -c_0^2 r & 0 & 0 & c_0^2 \\ 0 & 0 & 0 & 0 \\ -\widetilde{\beta} u & \widetilde{\beta} & 0 & 0 \end{bmatrix}, \boldsymbol{S}(\boldsymbol{U}) = \begin{bmatrix} 0 \\ Q\partial_x b - fhv \\ fhu \\ \alpha hr \end{bmatrix}$$

- Hyperbolicity determined by eigenstructure (all eigenvalues must be real). Eigenvalues of the system are determined by the Jacobian matrix:

$$\partial \boldsymbol{F}/\partial \boldsymbol{U} + \boldsymbol{G}(\boldsymbol{U}) = \begin{bmatrix} 0 & 1 & 0 & 0 \\ -u^2 - c_0^2 r + \partial_h P & 2u & 0 & c_0^2 \\ -uv & v & u & 0 \\ -u(\widetilde{\beta} + r) & \widetilde{\beta} + r & 0 & u \end{bmatrix},$$

and its four eigenvalues are:

$$\lambda_{1,2} = u \pm \sqrt{\partial_h P + c_0^2 \widetilde{\beta}}, \quad \lambda_{3,4} = u.$$

- Since $P(h;b)$ is non-decreasing and $\widetilde{\beta}$ non-negative, the eigenvalues are real.

DGFEM for modRSW

- TASK: convert the PDE of interest into its equivalent weak formulation using the standard test function and integration approach
- PROBLEM: the presence of NCPs in the governing equations complicates this somewhat because the weak solution in the classical sense of distributions does not exist when the solution becomes discontinuous
- SOLUTION: to overcome the absence of a weak solution, Rhebergen et al. (2008) employ DLM theory (after Dal Maso, LeFloch, and Murat 1995) for NCPs which defines an NCP as a bounded measure in such a way to enable the weak solution to be defined. This is achieved by considering a single NCP $g(u)\partial_x u$, where g is a smooth function but u may admit discontinuities, and defining a smooth regularization u^ϵ of the discontinuous u:

$$g(u)\frac{\mathrm{d}u}{\mathrm{d}x} \equiv \lim_{\epsilon\to 0} g(u^\epsilon)\frac{\mathrm{d}u^\epsilon}{\mathrm{d}x} = C\delta_{x_d}, \text{ with } C = \int_0^1 g(\phi(\tau))\frac{\partial\phi}{\partial\tau}(\tau)\mathrm{d}\tau,$$

where δ_{x_d} is the Dirac measure at the discontinuity x_d and ϕ is a Lipschitiz continuous path connecting the model states across the discontinuity, an artefact of the regularization.

- The one-dimensional flow domain $\Omega = [0, L]$ is divided into N open elements $K_k = (x_k, x_{k+1})$ for $k = 1, 2, ..., N$ with $N + 1$ nodes/edges $0 = x_1, x_2, ..., x_N, x_{N+1} = L$. Element lengths $|K_k| = x_{k+1} - x_k$ may vary.
- space-DGFEM weak formulation is obtained by (i) multiplying the each equation of the system by an arbitrary test function $w \in C^1(K_k)$, generally continuous on each element but discontinuous across an element boundary; and (ii) integrating (by parts) over each element $K_k \in \mathcal{T}_h$ and summing over all elements. The space discretisation is achieved by replacing the exact model states $\boldsymbol{U}$ and test functions w by approximations $\boldsymbol{U}_h, w_h$ in terms of polynomial basis function expansions, with the order of the polynomials determining the order of the scheme
- In one space dimension and considering cell K_k only at a given t, the weak form reads:

$$0 = \int_{K_k} [w\partial_t U_i - F_i \partial_x w + w G_{ij} \partial_x U_j + w S_i] \, \mathrm{d}x$$
$$+ \left[w(x_{k+1}^L) \mathcal{P}_i^p (\boldsymbol{U}_{k+1}^L, \boldsymbol{U}_{k+1}^R) - w(x_k^R) \mathcal{P}_i^m (\boldsymbol{U}_k^L, \boldsymbol{U}_k^R) \right],$$

where $\mathcal{P}_i^p$ and $\mathcal{P}_i^m$ are the numerical flux terms given by:

$$\mathcal{P}_i^p = \mathcal{P}_i^{NC} + \frac{1}{2} \int_0^1 G_{ij}(\boldsymbol{\phi}) \frac{\partial \phi_j}{\partial \tau} \mathrm{d}\tau,$$
$$\mathcal{P}_i^m = \mathcal{P}_i^{NC} - \frac{1}{2} \int_0^1 G_{ij}(\boldsymbol{\phi}) \frac{\partial \phi_j}{\partial \tau} \mathrm{d}\tau,$$

- ... and the NCP flux through an element edge is:

$$\mathcal{P}_i^{NC}(\boldsymbol{U}^L,\boldsymbol{U}^R) = \begin{cases} F_i^L - \frac{1}{2}\int_0^1 G_{ij}(\boldsymbol{\phi})\frac{\partial\phi_j}{\partial\tau}\mathrm{d}\tau, & \text{if } S^L > 0; \\ F_i^{HLL} - \frac{1}{2}\frac{S^L+S^R}{S^R-S^L}\int_0^1 G_{ij}(\boldsymbol{\phi})\frac{\partial\phi_j}{\partial\tau}\mathrm{d}\tau, & \text{if } S^L < 0 < S^R; \\ F_i^R + \frac{1}{2}\int_0^1 G_{ij}(\boldsymbol{\phi})\frac{\partial\phi_j}{\partial\tau}\mathrm{d}\tau, & \text{if } S^R < 0. \end{cases}$$

- Here, F_i^{HLL} is the standard HLL numerical flux,

$$F_i^{HLL} = \frac{F_i^L S^R - F_i^R S^L + S^L S^R (U_i^R - U_i^L)}{S^R - S^L},$$

G_{ij} is the ij-th element of the matrix $\boldsymbol{G}$, and $S^{L,R}$ are the fastest left- and right-moving signal velocities in the solution of the Riemann problem, determined by the eigenvalues of the Jacobian of the system:

$$S^L = \min\left(u^L - \sqrt{(\partial_h P)|^L + c_0^2\widetilde{\beta}|^L}, u^R - \sqrt{(\partial_h P)|^R + c_0^2\widetilde{\beta}|^R}\right),$$

$$S^R = \max\left(u^L + \sqrt{(\partial_h P)|^L + c_0^2\widetilde{\beta}|^L}, u^R + \sqrt{(\partial_h P)|^R + c_0^2\widetilde{\beta}|^R}\right).$$

Steady-state modRSW solutions

Consider a system of equations for h, u, and r:

$$
\begin{aligned}
&\partial_t h + \partial_x (hu) = 0, \\
&\partial_t u + u\partial_x u + \partial_x \Phi = 0, \\
&\partial_t r + u\partial_x r + \widetilde{\beta}\partial_x u + \alpha r = 0,
\end{aligned}
$$

where:

$$
\Phi = \begin{cases} \Phi_c + c_0^2 r, & \text{for } h + b > H_c, \\ g(h+b) + c_0^2 r, & \text{otherwise.} \end{cases}
$$

Steady-state solutions are found by considering time-independent flow ($\partial_t(\cdot) = 0$):

$$
\begin{aligned}
&\partial_x (hu) = 0, \\
&u\partial_x u + \partial_x \Phi = 0, \\
&u\partial_x r + \widetilde{\beta}\partial_x u + \alpha r = 0,
\end{aligned}
$$

The first of these steady-state equations gives immediately a solution of u in terms of h:

$$\partial_x(hu) = 0 \implies hu = K, \text{ for constant } K \implies u = \frac{K}{h},$$

which is then substituted into the remaining equations, yielding a system of 2 ODEs to solve for h and r:

$$-\frac{K^2}{h^3}\partial_x h + \partial_x \Phi = 0,$$
$$\frac{K}{h}\partial_x r - \frac{K}{h^2}\widetilde{\beta}\partial_x h + \alpha r = 0.$$

We seek a system of the form $\boldsymbol{M}\boldsymbol{X}' = \boldsymbol{Y}$, where $\boldsymbol{X} = (h, r)^T$, prime denotes derivative with respect to x, and $\boldsymbol{M} \in \mathbb{R}^{2\times 2}$, $\boldsymbol{Y} \in \mathbb{R}^2$ are given from the equations set. If $\boldsymbol{M}$ is non-singular (and hence invertible), then we can solve $\boldsymbol{X}' = \boldsymbol{M}^{-1}\boldsymbol{Y}$ numerically for $\boldsymbol{X}$ using, e.g., a simple finite difference scheme.

The system is expanded as follows:

$$\left[-\frac{K^2}{h^3}+g|_{H_c}\right]\partial_x h+\left[c_0^2\right]\partial_x r=-\left[g|_{H_c}\partial_x b\right],$$
$$\left[\frac{K}{h}\right]\partial_x r-\left[\frac{K}{h^2}\widetilde{\beta}\right]\partial_x h=-\left[\alpha r\right],$$

where $g|_{H_c}=g$ if $h+b\leq H_c$ and zero otherwise and the terms in square brackets are components of $\boldsymbol{M}$ and $\boldsymbol{Y}$:

$$\boldsymbol{M}=\begin{bmatrix}-\frac{K^2}{h^3}+g|_{H_c} & c_0^2\\ -\frac{K}{h^2}\widetilde{\beta} & \frac{K}{h}\end{bmatrix},\quad \boldsymbol{Y}=\begin{bmatrix}-g|_{H_c}\partial_x b\\ -\alpha r\end{bmatrix}.$$

The $\widetilde{\beta}$ term requires further manipulation; re-writing in terms of the Heaviside function we have:

$$\begin{aligned}\widetilde{\beta}&=\beta\Theta(-\partial_x u)\Theta(h+b-H_r)\\&=\beta\Theta(K/h^2\partial_x h)\Theta(h+b-H_r),\\&=\beta\Theta(\partial_x h)\Theta(h+b-H_r).\end{aligned}$$

Thus, the system reads $\boldsymbol{X}'=f(\boldsymbol{X})$ where $f(\boldsymbol{X})=\boldsymbol{M}^{-1}\boldsymbol{Y}$ and is solved using, e.g., a forward Euler finite difference scheme: $\boldsymbol{X}^{j+1}=\boldsymbol{X}^j+\triangle x f(\boldsymbol{X}^j,\boldsymbol{X}^{j-1})$. The value at $j-1$ is required to compute the Heaviside of the height gradient; all other components in $f(\boldsymbol{X})=\boldsymbol{M}^{-1}\boldsymbol{Y}$ are evaluated using values at level j. To start marching through space, note that $\boldsymbol{X}^1=\boldsymbol{X}^2$, so that $\widetilde{\beta}=0$. Then proceed as usual for $j\geq 1$.